Bulletin of Faculty of Science, Zagazig University (BFSZU)
e-ISSN: 1110-1555
Volume-2025, Issue-4, pp-42-53
https://bfszu.journals.ekb.eg/journal
Research Paper DOI: **10.21608/bfszu.2025.349351.1473**

==========

Petrophysical Analysis of Abu Roash Formation using well log data, Khalda oil field, North Western Desert, Egypt

Mohamed A. Kamel [1, *], Ashraf Ghoneimi [1], Muhammed Nabih [1], Ibrahim M. Al-Alfy [2].

[1]Faculty of Science, Zagazig University, 44519, Zagazig, Egypt
[2]Exploration Division, Nuclear Materials Authority, P.O. 530, Kattameya, Cairo, Egypt
***Corresponding autho**r: Mohamed.saleh9@yahoo.com (Mohamed Adel Kamel)

***ABSTRACT*: Khalda oil field lies in the Shushan basin in the northern Western Desert. Abu Roash Formation (AR) is this concession's targeted hydrocarbon exploration unit. This study inspects the formation's petrophysical parameters by interpreting the log data of three wells namely, KH-21, KH-17, and KH-24. Abu Roash Formation, within Cenomanian (G), mostly Turonian (F, E, D, C and B), and Coniacian/Santonian (A), consists of limestone, dolomite, and shale that varies along the Formation. The results of petrophysical analysis reveal variations in shale volume, effective porosity, and water saturation. This study evaluates hydrocarbon-bearing zones within the Abu Roash Formation in the Western Desert, Egypt, offering valuable insights into the reservoir characteristics of the formation. The correlation section illustrates the vertical distribution of effective porosity (PHIE) and hydrocarbon saturation (Sh) across three wells, KH-21, KH-17, and KH-24 highlighting significant variations in reservoir quality and hydrocarbon potential. The petrophysical analysis reveals hydrocarbon-bearing intervals within the Abu Roash Formation specifically in AR-A, AR-B1, AR-B2, AR-D, and AR-F2 in KH-21 well. These intervals demonstrate promising reservoir characteristics, including low water saturation and high hydrocarbon potential, highlighting their significance as key targets for further exploration and development.**

KEYWORDS: Abu Roash Formation; Western Desert of Egypt; Well log analysis; Hydrocarbon potential evaluation; Khalda oil field.

Date of Submission: 28-01-2025 Date of acceptance: 23-03-2025

I. INTRODUCTION

The northern Western Desert in Egypt has the most prolific petroleum province after the Red Sea region, where it comprises a considerable number of significant petroleum basins such as Alamein Basin, Matruh-Shushan Basin, Faghur Basin, Gindi Basin, Abu Gharadig Basin as shown in Figure 1. The Abu Roash Formation, a key target for hydrocarbon exploration, plays a significant role in this context. Hydrocarbon occurrence in the Western Desert is closely related to the area's tectonic activities and stratigraphic history, which has created a series of reservoirs and seals [1]. The Khalda oil field represents the central region of the Khalda concession area and is located in the northern section of the Shushan Basin.

Estimations by core samples which are costly and time-intensive provide precise reservoir parameters, including pore fluid, porosity, permeability, and lithology, requiring substantial effort to give meaningful data [2]. Drilling cuttings also offer insights into reservoir characteristics and their limited size frequently impedes accuracy and reliability [3]. Therefore, well log data is an affordable and efficient method for assessing reservoir characteristics. Well logging covers the full extent of the target geological formation and provides comprehensive and essential information about subsurface characteristics.

Well log analysis plays a pivotal role in understanding reservoir characteristics. By estimating the principle petrophysical parameters such as shale volume, effective porosity, water saturation, and hydrocarbon saturation, and so identification of the reservoir potential zones. Shale volume distinguishes between reservoir and non-reservoir zones, while effective porosity and fluid saturation give insight on the reservoir fluid type and pore space volume, leading to the identification of hydrocarbon-bearing intervals. In this study, we demonstrate the practicality and efficiency of well log data analysis, highlighting its crucial role in the exploration and evaluation of hydrocarbon reservoirs. Reservoir characterization in the North Western Desert of Egypt requires

a multi-disciplinary approach integrating well log data, statistical analysis, and petrophysical parameters to enhance the prediction of reservoir quality and hydrocarbon potential [4]. In this paper, the interpretation of well log data reveals hydrocarbon-bearing intervals particularly in AR-A, AR-B1, AR-B2, AR-D, and AR-F2 within the KH-21 well. These zones exhibit favorable reservoir properties.

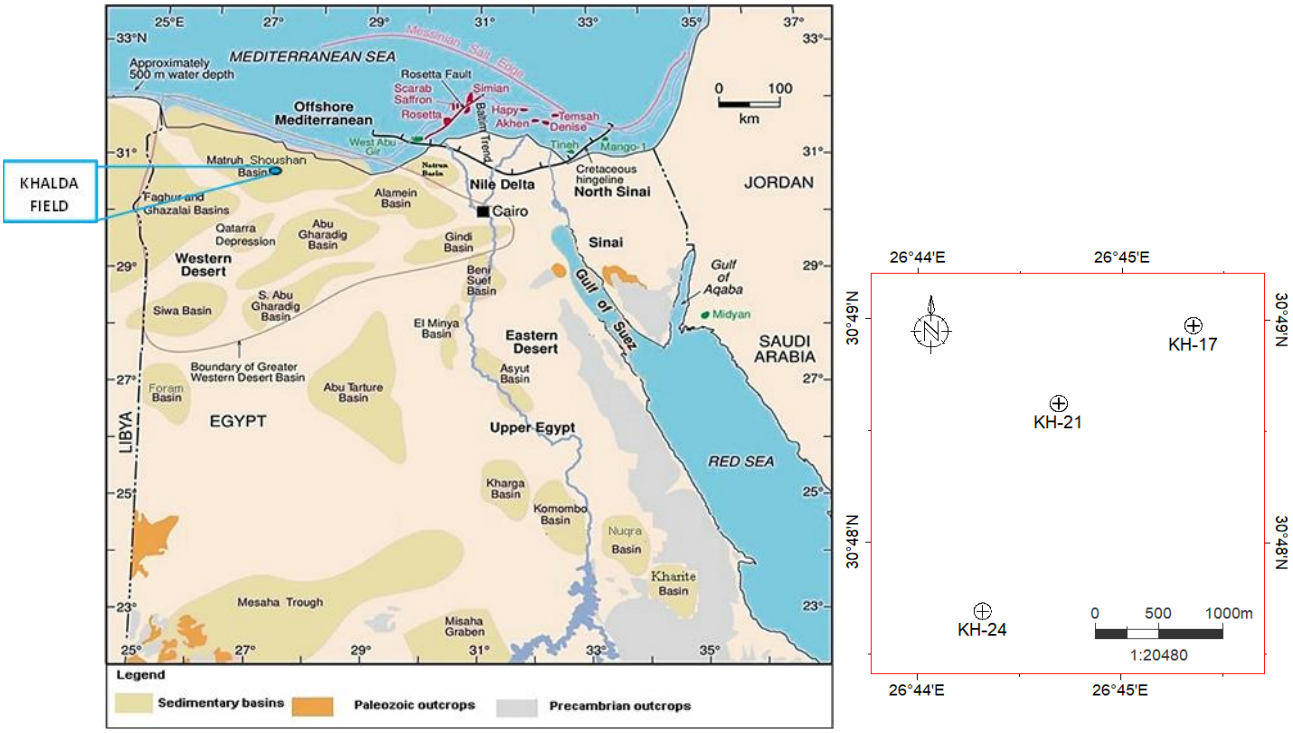

Figure 1. (a) A map showcasing the study area [10]. (b) A map emphasizing the locations of three wells situated within the Khalda oil field in Egypt's Western Desert.

II. GEOLOGICAL SETTING

The Shushan Basin has a rich geological history, having evolved under significant tectonic activities, primarily during the Mesozoic era. The initial rifting in the Western Desert, which occurred in the Late Triassic, was followed by major phases during the Middle Jurassic [5]. The region's tectonics were shaped by the opening of the Neo-Tethys Ocean and subsequent compressive events, such as the Syrian Arc deformation during the Late Cretaceous. This compressive phase resulted in the inversion of earlier extensional basins, creating numerous structural traps suitable for hydrocarbon accumulation. Understanding this historical context is crucial for comprehending the current geological complexity and hydrocarbon trapping mechanisms of the Shushan Basin.

Moreover, the Shushan Basin underwent significant thermal subsidence during the post-rift phases, particularly during the Albian to Coniacian periods (Figure 2). This was associated with heat flux and crustal stretching, which enhanced its petroleum potential by creating thick sedimentary sequences with source rock maturation [6]. The tectonic evolution of the Shushan Basin was also influenced by the regional compressional stresses caused by the convergence of the African and Eurasian plates. This resulted in the developing NE-ENE trending folds and fault systems, enhancing its geological complexity and hydrocarbon trapping mechanisms [7].

Rifting events during the Jurassic and Cretaceous periods established the primary basin architecture. These events were accompanied by volcanism, contributing to the deposition of siliciclastic and carbonate rocks that form key source and reservoir units in the basin [8]. The faulted anticlines and horst-graben structures dominate the basin's architecture, significantly influenced by Jurassic and Cretaceous extensional faulting and subsequent compressional tectonics. These tectonic regimes facilitated the formation of tilted fault block traps and compressional folds, crucial for hydrocarbon entrapment [9].

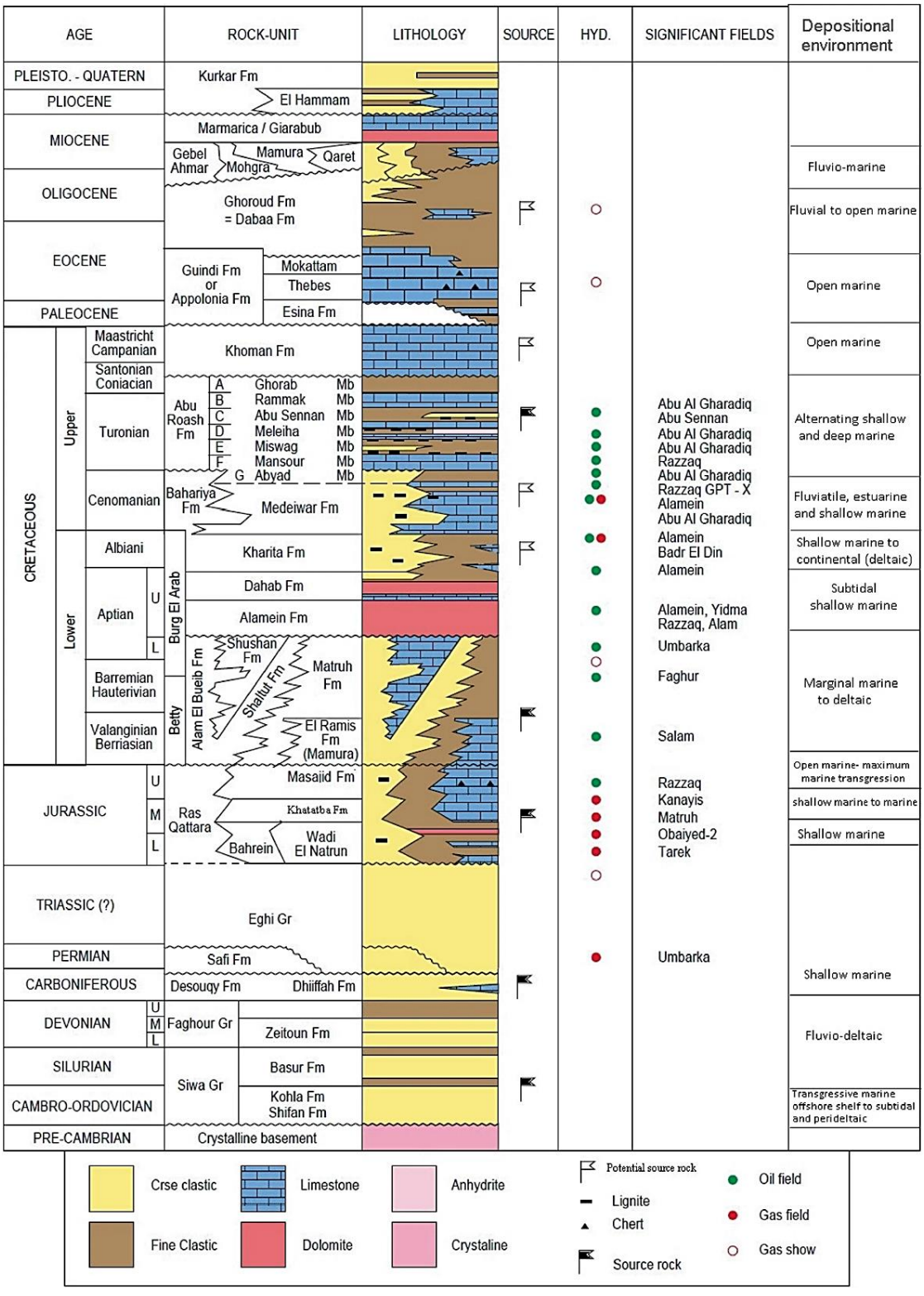

Figure 2. A Stratigraphic column of the northern Western Desert highlighting the major source rocks, reservoir units, and key hydrocarbon-producing Formations [10].

Khalda oil field is close to the Shushan basin's northern boundary, which rapidly declined throughout the Jurassic and Early Cretaceous periods. In the Shushan Basin, the post-rift Upper Cretaceous sequence is defined by siliciclastic facies that shift from continental to coastal environments in the Kharita and Bahariya formations, progressing upward to marine carbonates found in the Abu Roash and Khoman formations in Figure 2 [10].

The Paleogene sequence is marked by marine carbonates of the Apollonia Formation at its base and marine siliciclastics of the Dabaa and Moghra formations at its upper levels [10]. Hydrocarbons are contained within structural traps in these basins aligned with the Syrian Arc structural trend SW-NE. These traps consist of fault blocks and structures with three-to-four-way closures, effectively sealing the hydrocarbons in place [11].

The Abu Roash Formation, the primary focus of this study in the Khalda field, is stratigraphically divided into seven members labeled from top to bottom as A, B, C, D, E, F, and G (Figure 2). These members range from the Turonian to upper Cenomanian ages [12]. The formation consists predominantly of chalky limestone interbedded with shale and sandstone layers, with a total thickness of approximately 217 meters at its type section, the Abu Roash-1 well, located in the northern Western Desert [13]. Stratigraphically, it is nearly conformable with the overlying Khoman Formation and rests on the Bahariya Formation. Palynological studies have confirmed its late Cenomanian-Turonian age [14]. Most of the facies within this formation were deposited under neritic to open marine conditions, except for the (G) member, which reflects deposition in lagoonal to mid-shelf environments [13].

III. MATERIALS AND METHODS

The primary purpose of well log analysis is to determine formation characteristics by estimating parameters such as shale volume, effective porosity, water saturation, and hydrocarbon saturation. The non-reservoirs from the reservoir intervals can be identified based on their Shale volume. Since shale is more radioactive than sandstone, its content is typically evaluated using gamma-ray logs [15,16]. The equations that relate shale volume to gamma-ray intensity were introduced by [17] as:

$$I_{GR} = \frac{GR\ log - GR\ min}{GR\ max - GR\ min} \qquad (1)$$

This can be modified to shale volume [18] using the equation for Tertiary (unconsolidated rocks):

$$V_{sh} = 0.083\ (2^{(3.7\ IGR)} - 1) \qquad (2)$$

where: I_{GR}: Gamma ray index, GR_{log}: Gamma ray reading at interest interval, GR_{min}: Minimum gamma ray (clean sand), GR_{max}: Maximum gamma ray (representing shale).
Assessing reservoir parameters relies heavily on effective porosity, a key parameter determined through the density-neutron crossplot. The calculation is governed by the following equations [19,20]:

$$\phi_{NC} = \phi_N - (V_{sh} * \phi_{N\,sh}) \qquad (3),$$

$$\phi_{DC} = \phi_D - (V_{sh} * \phi_{D\,sh}) \qquad (4), \text{ and}$$

$$\phi_e = \sqrt{\frac{(\phi DC)^2 + (\phi NC)^2}{2}} \qquad (5).$$

Here: ϕ_{NC} = Corrected neutron porosity, ϕ_N = Neutron porosity, ϕ_{Nsh} = Apparent neutron porosity in shale, V_{sh} = Shale volume, ϕ_{DC} = Corrected density porosity, ϕ_D = Density porosity, ϕ_{Dsh} = Apparent density porosity in shale, ϕ_e = Effective porosity.
Estimations of fluid saturation, the first step is to differentiate between the various fluid types whether oil or water. The archie equation is employed to calculate water saturation [21].

$$S_w{}^n = \frac{a \times Rw}{\phi^m \times R_t} \qquad (6)$$

Where: Sw is the water saturation, n is the saturation exponent, a is the tortuosity factor, Rw is the resistivity of formation water, (ohm-m), ϕ is the porosity, m is the cementation factor, Rt is the true formation resistivity (ohm-m). The hydrocarbon saturation is subsequently estimated using the following equation:

$$S_h = 1 - S_w \qquad (7).$$

By applying suitable cutoffs, zones saturated with hydrocarbons are recognized by meeting specific cut offs: effective porosity above 10%, hydrocarbon saturation over 50%, and shale volume less than 35%. These values of conventional well log analysis are essential for pinpointing oil-bearing intervals.

IV. RESULTS AND DISCUSSION

Well Log interpretation in KH-21 well (Figure 3) of Abu Roash Formation showed average effective porosity, water saturation, and e clay volume as illustrated in Table 1. In KH-21 well, the zones exhibit varying characteristics like zone AR-A (3736–3920 ft) has an average clay volume of 14%, effective porosity of 22%, and water saturation of 62%. While it meets the clay volume and porosity cutoffs, the hydrocarbon saturation is below 50%, indicating limited productivity. Zone AR-B1 (3920–4228 ft) consists of 10% clay, 22% effective porosity, and 58% water saturation. Despite favorable porosity and clay content, low hydrocarbon saturation restricts its potential. Zone AR-B2 (4228–4639 ft) has 7% clay, 20% porosity, and 65% water saturation. Although the porosity and clay volume meet the thresholds, the hydrocarbon saturation falls below the required cutoff. Zone AR-C (4639–4790 ft) has 21% clay, 23% porosity, and 56% water saturation. This zone meets the porosity and clay cutoffs but remains marginal due to low hydrocarbon saturation. Zone AR-D (4790–5122 ft) consists of 7% clay, 20% porosity, and 62% water saturation. While it satisfies the clay volume requirement, its porosity and hydrocarbon saturation fall short, indicating poor productivity. Zone AR-E (5122–5198 ft) has 17% clay, 23% porosity, and 54% water saturation. Although the clay content is within acceptable limits, low hydrocarbon saturation reduces its viability. Zone AR-F1 (5198–5418 ft) includes 19% clay, 23% porosity, and 64% water saturation. Despite favorable porosity and clay content, insufficient hydrocarbon saturation limits its productivity. Zone AR-F2 (5418–5629 ft) has 12% clay, 21% porosity, and 53% water saturation. While the clay content and porosity meet the cutoffs, hydrocarbon saturation remains below the required level. Zone AR-G (5629–6214 ft) has 29% clay, 20% porosity, and 59% water saturation. This zone satisfies the clay volume requirement but fails to meet the hydrocarbon saturation and porosity cutoffs, indicating low potential.

In KH-17 well of Abu Roash Formation showed mean effective porosity, mean water saturation, and mean clay volume as illustrated in Table 2. In KH-17 well, zone AR-A (3945–4068 ft) has 15% clay, 19% porosity, and 51% water saturation. This zone meets all cutoffs, indicating good hydrocarbon potential. Zone AR-B1 (4068–4388 ft) has 11% clay, 22% porosity, and 63% water saturation. While the clay content and porosity are favorable, hydrocarbon saturation remains below 50%, reducing its attractiveness. Zone AR-B2 (4388–4809 ft) shows 7% clay, 23% porosity, and 68% water saturation. Despite meeting the clay and porosity thresholds, insufficient hydrocarbon saturation limits productivity. Zone AR-C (4809–4961 ft) has 21% clay, 23% porosity, and 56% water saturation. Although the clay content and porosity are acceptable, hydrocarbon saturation does not meet the cutoff, making it marginally productive. Zone AR-D (4961–5328 ft) consists of limestone with 8% clay, 21% porosity, and 66% water saturation. While clay volume is favorable, porosity and hydrocarbon saturation remain below the thresholds, indicating poor productivity. Zone AR-E (5328–5438 ft) shows 12% clay, 20% porosity, and 55% water saturation. Despite meeting the clay and porosity cutoffs, hydrocarbon saturation is insufficient for commercial productivity. Zone AR-F1 (5438–5671 ft) has 15% clay, 22% porosity, and 65% water saturation. While porosity and clay content are within limits, low hydrocarbon saturation reduces its potential. Zone AR-F2 (5671–5882 ft) consists of 12% clay, 18% porosity, and 56% water saturation. The clay volume is favorable, but the porosity and hydrocarbon saturation do not meet the required thresholds, indicating limited productivity. Zone AR-G (5882–6421 ft) exhibits 27% clay, 20% porosity, and 57% water saturation. Although it satisfies the clay volume requirement, its hydrocarbon saturation and porosity fall below the cutoffs, making it marginally productive.

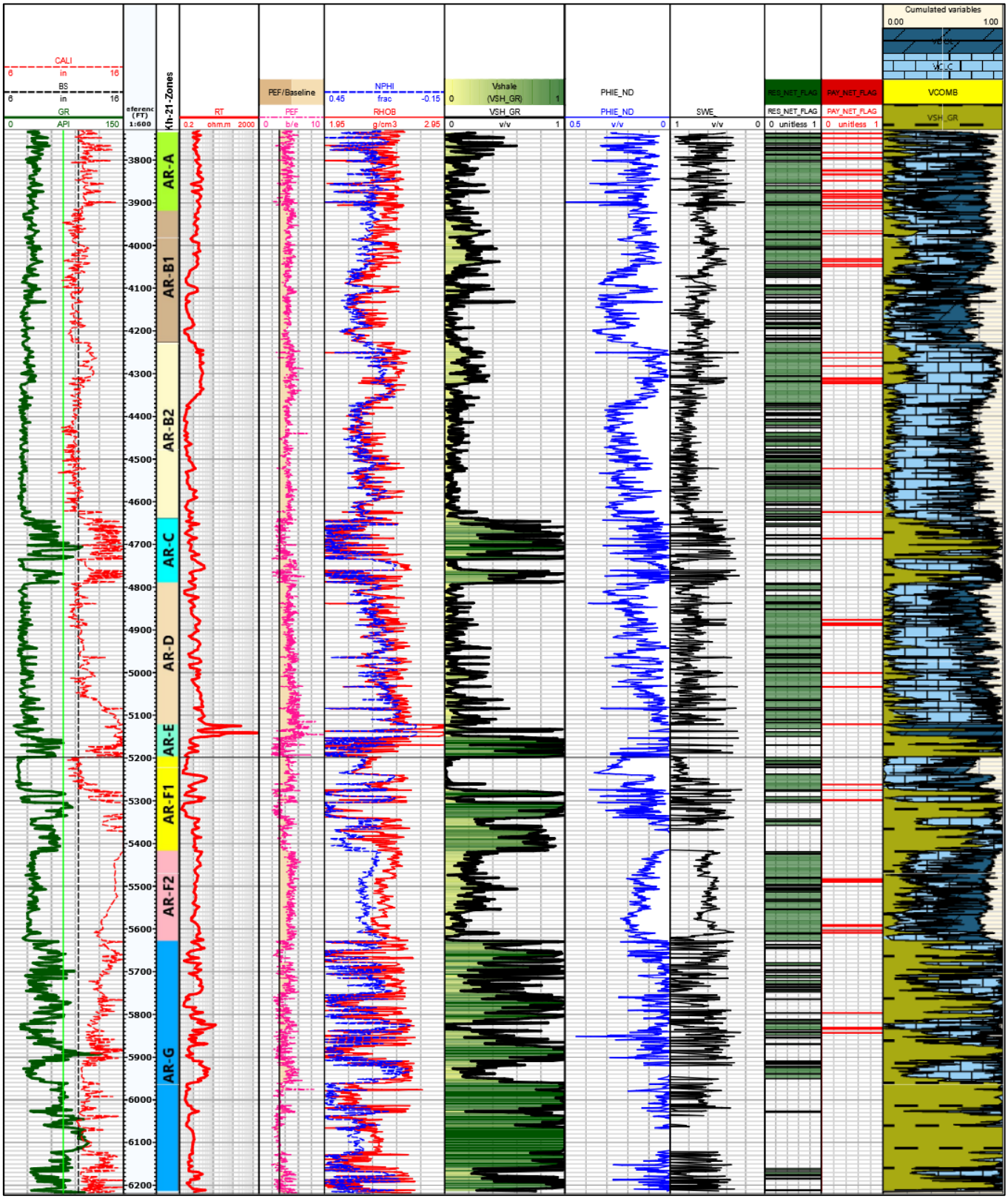

Figure 3. Petrophysical analysis of Abu Roash Formation in KH-21 well showing lithology, shale volume (Vsh), effective porosity (PHIE), and net pay.

Table 1. Petrophysical parameters of Abu Roash Formation in KH-21 well.

Zones	Top (ft)	Lithology	Average clay volume (%)	Average effective porosity (%)	Average water saturation (%)	Average hydrocarbon saturation (%)
AR_A	3736	Shaly Lst.	14%	22%	62%	38%
AR_B1	3920	Lst.	10%	22%	58%	42%
AR_B2	4228	Lst.	7%	20%	65%	35%
AR_C	4639	Sandy Shale	21%	23%	56%	44%
AR_D	4790	Lst.	7%	20%	62%	38%
AR_E	5122	Silty Shale	17%	23%	54%	46%
AR_F1	5198	Shaly Lst.	19%	23%	64%	36%
AR_F2	5418	Lst.	12%	21%	53%	47%
AR_G	5629	Sandy Shale	29%	20%	59%	41%

Table 2. Petrophysical parameters of Abu Roash Formation in KH-17 well.

Zones	Top (ft)	Lithology	Average clay volume (%)	Average effective porosity (%)	Average water saturation (%)	Average hydrocarbon saturation (%)
AR_A	3945	Shaly Lst.	15%	19%	51%	49%
AR_B1	4068	Lst.	11%	22%	63%	37%
AR_B2	4388	Lst.	7%	23%	68%	32%
AR_C	4809	Sandy Shale	21%	23%	56%	44%
AR_D	4961	Lst.	8%	21%	66%	34%
AR_E	5328	Silty Shale	12%	20%	55%	45%
AR_F1	5438	Shaly Lst.	15%	22%	65%	35%
AR_F2	5671	Lst.	12%	18%	56%	44%
AR_G	5882	Sandy Shale	27%	20%	57%	43%

In KH-24 well of Abu Roash Formation in Table 3, Zone AR-A (3962–4140 ft) has 13% clay, 16% porosity, and 55% water saturation. Despite favorable clay content, marginal porosity and low hydrocarbon saturation limit productivity. Zone AR-B1 (4140–4502 ft) consists of 6% clay, 21% porosity, and 67% water saturation. Although lithology is clean and porosity is excellent, insufficient hydrocarbon saturation precludes productivity. Zone AR-B2 (4502–4860 ft) features 5% clay, 20% porosity, and 68% water saturation. Similar to AR-B1, this zone exhibits excellent porosity and minimal clay volume, but hydrocarbon saturation remains below 50%. Zone AR-C (4860–4992 ft) has 22% clay, 19% porosity, and 57% water saturation. While clay volume and porosity meet the cutoffs, hydrocarbon saturation does not, making it marginally productive. Zone AR-D (4992–5133 ft) consists of 7% clay, 16% porosity, and 64% water saturation. Both porosity and hydrocarbon saturation fall below the required thresholds, making this zone unproductive. Zone AR-E (5133–

5248 ft) has 16% clay, 14% porosity, and 50% water saturation. While clay content is within limits, both porosity and hydrocarbon saturation are insufficient, limiting productivity. Zone AR-F1 (5248–5489 ft) consists of 17% clay, 20% porosity, and 68% water saturation. Despite excellent porosity and acceptable clay content, hydrocarbon saturation remains low. Zone AR-F2 (5489–5695 ft) features 6% clay, 15% porosity, and 64% water saturation. Similar to AR-D, this zone does not meet the porosity or hydrocarbon saturation cutoffs, making it unproductive. Zone AR-G (5695–6243 ft) exhibits 27% clay, 20% porosity, and 57% water saturation. While porosity and clay volume are within acceptable ranges, hydrocarbon saturation remains below the required threshold, resulting in low productivity.

Table 3. Petrophysical parameters of Abu Roash Formation in KH-24 well.

Zones	Top (ft)	Lithology	Average clay volume (%)	Average effective porosity (%)	Average water saturation (%)	Average hydrocarbon saturation (%)
AR_A	3962	Shaly Lst.	13%	16%	55%	45%
AR_B1	4140	Lst.	6%	21%	67%	33%
AR_B2	4502	Lst.	5%	20%	68%	32%
AR_C	4860	Sandy Shale	22%	19%	57%	43%
AR_D	4992	Lst.	7%	16%	64%	36%
AR_E	5133	Silty Shale	16%	14%	50%	50%
AR_F1	5248	Shaly Lst.	17%	20%	68%	32%
AR_F2	5489	Lst.	6%	15%	64%	36%
AR_G	5695	Sandy Shale	27%	20%	57%	43%

Across the three wells, the well log analysis indicates that while several zones across the three wells meet the porosity and clay content cutoffs. The primary hydrocarbon-bearing intervals are observed in the Abu Roash Formation (AR-A, AR-B1, AR-B2, AR-D, and AR-F2). These intervals exhibit characteristics of hydrocarbon saturation with low water saturation and favorable reservoir properties. Further testing is recommended to confirm these findings.

The histograms show the clay volume distribution (Vsh), effective porosity distribution (PHIE), and hydrocarbon saturation distribution (Sh) of Abu Roash Formation through the three wells at Khalda oil field in Figure 4.

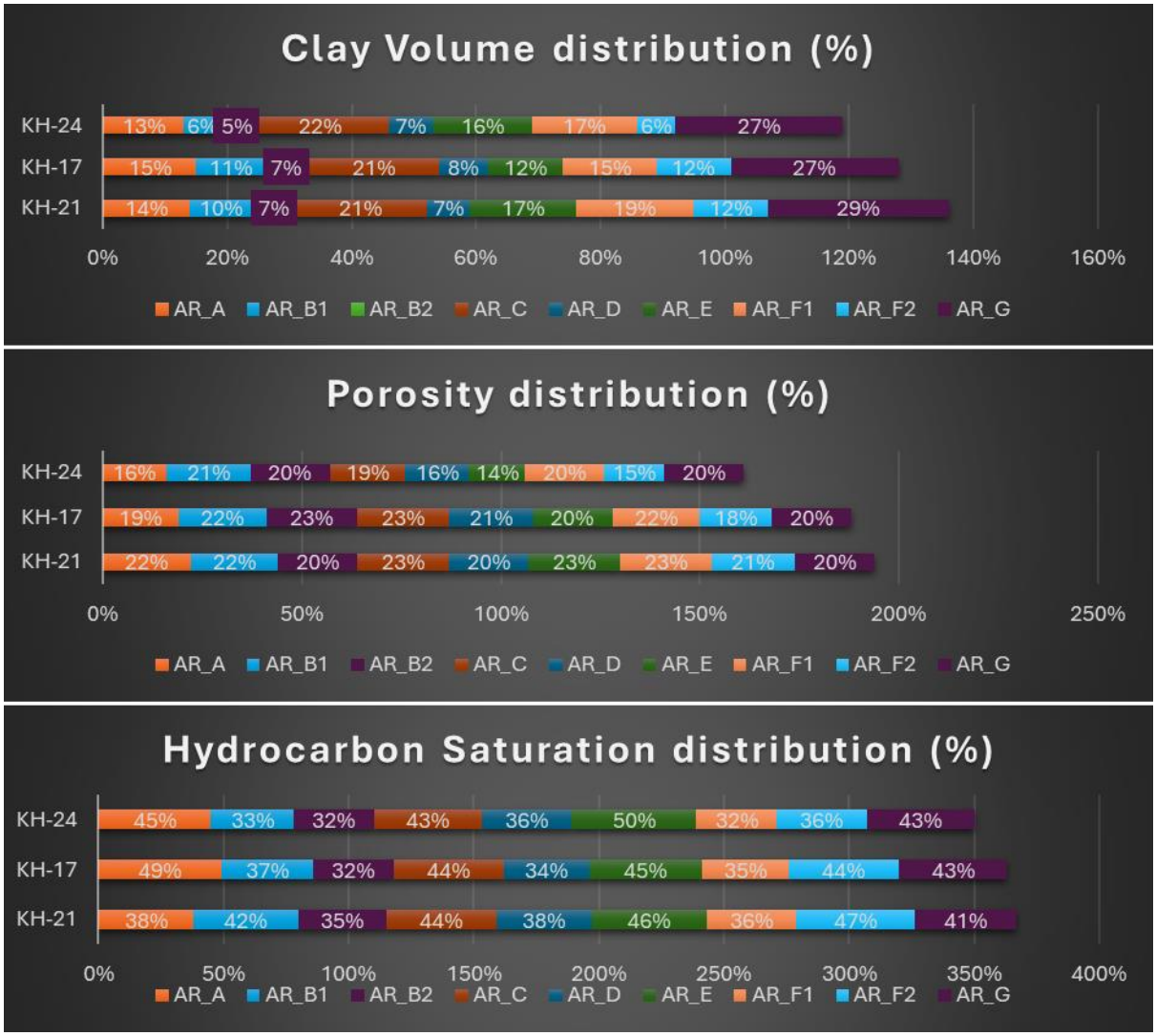

Figure 4. Histograms show the clay volume distribution (Vsh), effective porosity distribution (PHIE), and hydrocarbon saturation distribution (Sh) of Abu Roash Formation through the three wells at Khalda oil field.

Correlation section among the three wells from SW (KH-24 well) to NE (KH-17 well) direction (Figure 5) shows a vertical distribution of the effective porosity as well as hydrocarbon saturation (Sh) in Abu Roash Formation at the three wells (KH-17, KH-21, and KH-24).

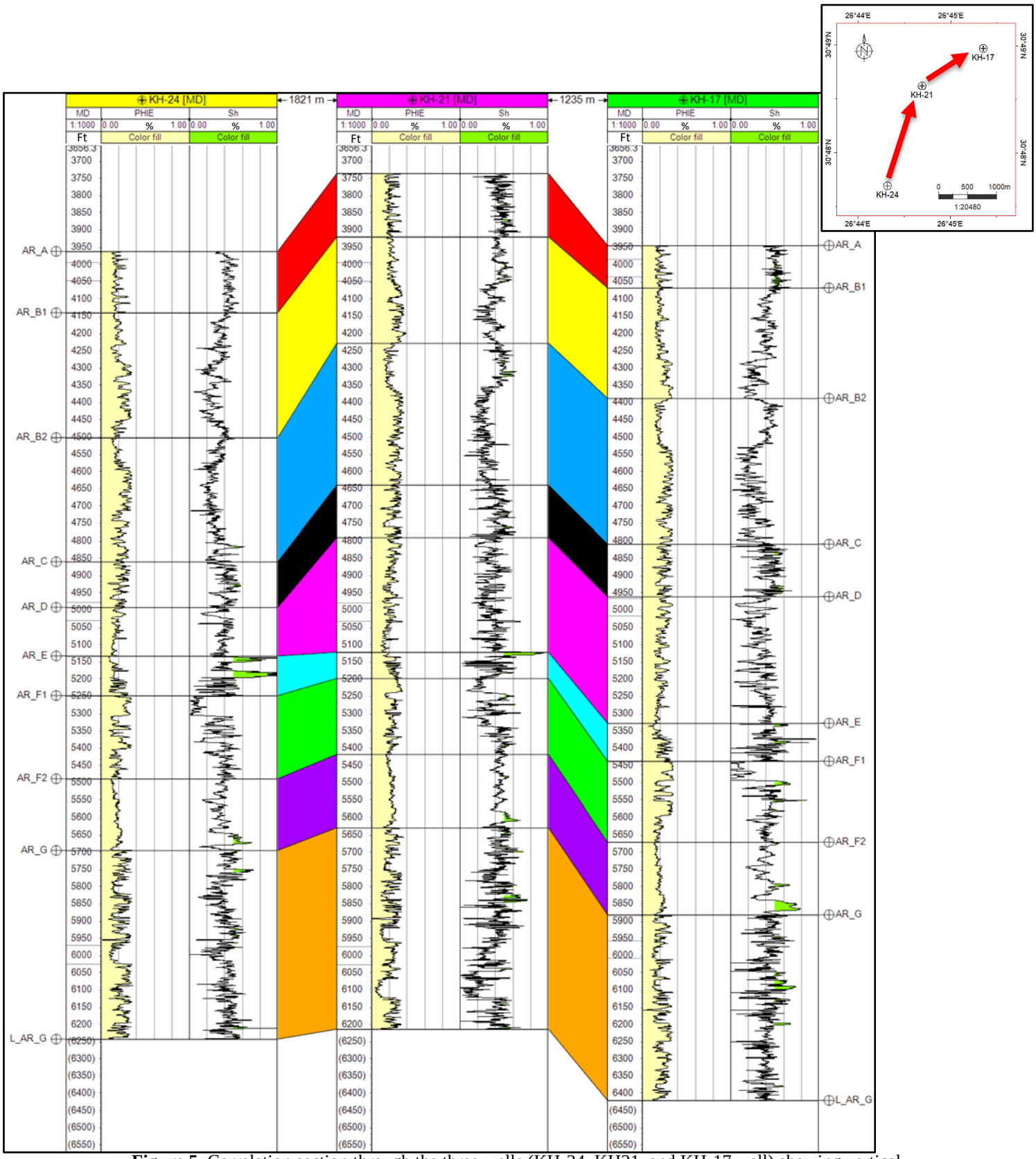

Figure 5. Correlation section through the three wells (KH-24, KH21, and KH-17 well) showing vertical distribution of the effective porosity (PHIE) and hydrocarbon saturation (Sh).

V. CONCLUSION

This study highlights and assess hydrocarbon-bearing zones within the Abu Roash Formation in the Western Desert, Egypt. It provides valuable insights into the reservoir characteristics of this Formation. Zones saturated with hydrocarbons are recognized by meeting specific cut offs like effective porosity above 10%, hydrocarbon saturation over 50%, and shale volume less than 35%.

The correlation section illustrates the vertical distribution of effective porosity (PHIE) and hydrocarbon saturation (Sh) across the three wells, providing insights into reservoir quality and hydrocarbon potential within the Abu Roash Formation. The petrophysical analysis indicates the presence of hydrocarbon-bearing intervals within Abu Roash Formation specifically in AR-A, AR-B1, AR-B2, AR-D, and AR-F2 in KH-21 well. These zones exhibit favorable reservoir properties with low water saturation and high hydrocarbon potential, making them key targets for further exploration and development.

CONFLICT OF INTEREST

The authors state that no conflict exists.

ACKNOWLEDGEMENT

Special thanks to the Academy of Scientific Research and Technology (ASRT) for awarding me a Master's Scholarship under the program "Scientists for Next Generation" (SNG) – Cycle 8, to the top graduates all over Egypt. This cycle honors the legacy of the late Professor Samia A. Temtamy, a pioneer in Human Genetics.

REFERENCES

[1] Abu El Naga, M., 1984. In Paleozoic and Mesozoic depocenters and hydrocarbon generating areas, in: 7th Petroleum and Exploration Seminar, Egyptian General Petroleum Corporation, Cairo Northern Western Desert.

[2] Chang, H.-C., Kopaska-Merkel, D.C., Chen, H.-C., 2002. Identification of lithofacies using Kohonen self-organizing maps. Comput Geosci 28, 223–229.

[3] Serra, O. t, Abbott, H.T., 1982. The contribution of logging data to sedimentology and stratigraphy. Society of Petroleum Engineers Journal 22, 117–131.

[4] Emad A Eysa, Fatma S Ramadan, Mohamed M El Nady, Nermin M Said (2016) Reservoir Characterization using Porosity – Permeability Relations and Statistical Analysis: A Case study from North Western Desert, Egypt. Arabian Journal of Geoscience 9(5): 403 doi.10.1007/s12517-016-2430-x.

[5] Radwan, A.E., 2023. Western desert petroleum system: New exploration opportunities and challenges. The Phanerozoic Geology and Natural Resources of Egypt 691–717.

[6] Metwalli, F.I., Pigott, J.D., 2005. Analysis of petroleum system criticals of the Matruh–Shushan Basin, Western Desert, Egypt. Petroleum Geoscience 11, 157–178.

[7] Guiraud, R., Bosworth, W., 1997. Senonian basin inversion and rejuvenation of rifting in Africa and Arabia: synthesis and implications to plate-scale tectonics. Tectonophysics 282, 39–82.

[8] Dolson, J.C., Shann, M. V, Matbouly, S., Harwood, C., Rashed, R., Hammouda, H., 2001. The Petroleum Potential of Egypt. Petroleum Provinces of the Twenty-First Century (AAPG Memoir 74, Chapter 23) 453–482.

[9] Abdelwahhab, M.A., Raef, A., 2020. Integrated reservoir and basin modeling in understanding the petroleum system and evaluating prospects: the Cenomanian reservoir, Bahariya Formation, at Falak Field, Shushan Basin, Western Desert, Egypt. J Pet Sci Eng 189, 107023.

[10] EGPC, 1992. production review (part 1), Western Desert, oil and gas fields, (a comprehensive overview). EGPC, Cairo 431.

[11] Nabawy, B.S., Abudeif, A.M., Masoud, M.M., Radwan, A.E., 2022. An integrated workflow for petrophysical characterization, microfacies analysis, and diagenetic attributes of the Lower Jurassic type section in northeastern Africa margin: Implications for subsurface gas prospection. Mar Pet Geol 140, 105678.

[12] Wever, H.E., 2000. Petroleum and source rock characterization based on C7 star plot results: Examples from Egypt. Am Assoc Pet Geol Bull 84, 1041–1054.

[13] Hantar, G., 1990. North-Western Desert, in: Said, R. (Ed.), The Geology of Egypt. A. A. Balkema, Rotterdam, Netherlands, 293–319.

[14] El Beialy, S.Y., El Atfy, H.S., Zavada, M.S., El Khoriby, E.M., Abu-Zied, R.H., 2010. Palynological, palynofacies, paleoenvironmental and organic geochemical studies on the Upper Cretaceous succession of the GPTSW-7 well, North-Western Desert, Egypt. Mar Pet Geol 27, 370–385.

[15] Abd Elaziz, M., Ghoneimi, A., Elsheikh, A.H., Abualigah, L., Bakry, A., Nabih, M., 2022. Predicting shale volume from seismic traces using modified random vector functional link based on transient search optimization model: A case study from Netherlands North Sea. Natural Resources Research 31, 1775–1791.

[16] Asquith, G., Krygowski, D., 2014. Basic Well Log Analysis, 2nd edition. AAPG Methods in Exploration Series, No. 16. American Association of Petroleum Geologists, Tulsa, Oklahoma.

[17] Dresser Atlas, 1979. Log Interpretation Charts. Dresser Industries, Houston, TX 107.

[18] Larionov, V. V, 1969. Radiometry of boreholes. Nedra, Moscow 127.

[19] Asquith, G., Krygowski, D., Henderson, S., Hurley, N., 2004. Basic well log analysis. American Association of Petroleum Geologists. https://doi.org/10.1306/Mth16823

[20] Bateman, R.M., 2012. Openhole Log Analysis and Formation Evaluation, Second Edition. Society of Petroleum Engineers (SPE).

[21] Archie, G. E. 1942. The electrical resistivity log as an aid in determining some reservoir characteristics. Transactions of the AIME 146(1), 54-62.